High-precision study of 2νββ of ^{130}Te from the CUORE experiment

Half-life & spectral-shape measurements

Stefano Dell'Oro, *on behalf of the CUORE Collaboration*

Dipartimento di Fisica G. Occhialini, Università di Milano-Bicocca

INFN, Sezione di Milano-Bicocca

XIX International Conference on Topics in Astroparticle and Underground Physics

August 24 - 30, 2025 – Xichang, Sichuan, China

Double Beta Decay: real and virtual neutrinos

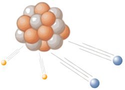

$$(A,Z) \rightarrow (A,Z{+}2) + 2e^- + 2\bar{\nu}_e \quad (2\nu\beta\beta)$$

$$(A,Z) \rightarrow (A,Z+2) \ + \ 2e^- \quad (0\nu\beta\beta)$$

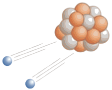

- 0νββ: creation of a pair of electrons
  - L-violation: discovery of 0νββ $\rightarrow$ L not a symmetry of the universe
    - link to baryon asymmetry in Universe (?)
  - key tool for studying neutrinos (3-ν exchange mechanism)
    - Majorana or Dirac nature + mass scale & ordering
- 2νββ: SM-allowed 2 nd-order nuclear process
  - observed in multiple nuclei with $T^{2\nu}_{1/2} \geqslant 10^{18}$ yr
  - tool for testing higher-order SM processes
  - experimental insights into nuclear structure
    - inform calculations for 0νββ mode

CUORE: Cryogenic Underground Observatory for Rare Events

- search for $0\nu\beta\beta$ of ^{130}Te
  - in data-taking at LNGS since April 2017
- largest cryogenic array ever built
  - 19 towers $\times$ 13 floors $\times$ 4 crystals = 988 detectors
  - 1 t detector mass: 327 kg Cu + 742 kg TeO_2

    $\rightarrow$ 206 kg of ^{130}Te

See talk by A. Campani

- latest limit on decay half-life
  - 2039 kg yr of TeO_2 / 567 kg yr of ^{130}Te
  - $t^{0\nu}_{1/2} > 3.5 \times 10^{25}$ yr @ 90% C. I.
  - $m_{\beta\beta} < (70 - 250)$ meV

Phys. Rev. Lett. 124, 122501 (2020) · Pending publication

Phys. Rev. Lett. 120, 132501 (2018) · Nature 604, 53 (2022)

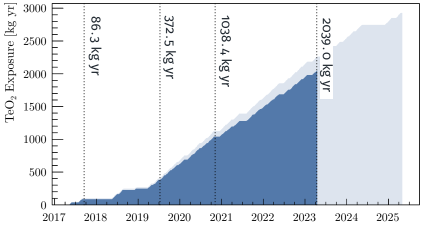

Operational performance

- year-long **cryogenic stability** at $T = 11 - 15$ mK
- uptime $>$**90%**
  - exposure rate $\sim$ 50 kg yr per month
- FWHM resolution at $Q_{\beta\beta}$ of **7.3 keV**
- bkg in ROI $\mathbf{1.4 \cdot 10^{-2}}$ **counts keV^{-1} kg^{-1} yr^{-1}**

CUORE background

Pending publication

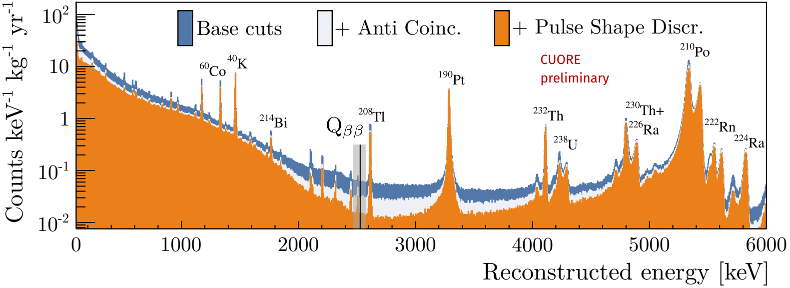

- different contributions in different regions of the energy spectrum
  - γ continuum + peaks up to 2.7 MeV
  - degraded α's in (2.7 — 3.9) MeV
  - α region from 4 MeV
- construction of an extensive **background model**
  - large effort ongoing since predecessors of CUORE
  - ultimate validation by CUORE data

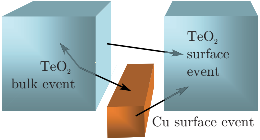

Modeling the background

- Geant4 simulation of contamination from different cryostat components
- background sources identified/ascribed to different locations in experimental setup
- **data-driven** Monte Carlo $\rightarrow$ inputs from
  - radio-assay measurements (HPGe, NAA, α spectroscopy)
  - modeling of CUORE-0 detector (single tower) Eur. Phys. J. C 77, 13 (2017)
  - CUORE data: α & γ peaks, time coincidences, event topologies
    - multiplicities ($\mathcal{M}$): exploit detector granularity

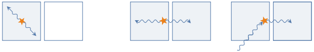

…

- raw Monte Carlo converted into CUORE-like data
  - include resolution, efficiencies, …

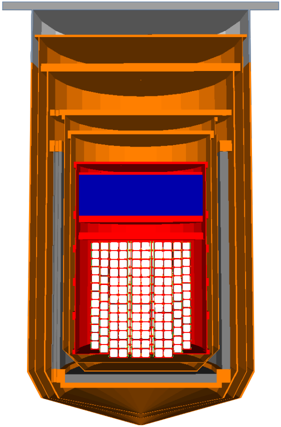

Fit to CUORE data

- validation dataset: 1038.4 kg yr of TeO_2
- simultaneous **Bayesian fit** to $\mathcal{M}1$, $\mathcal{M}2$ energy spectra
  - $\sim$ **80 parameters** to describe contamination sources
    - bulk and surface (different depths)
  - Gaussian / expontial prior distributions from input values / limits
  - energy range from 200 keV to 6.8 MeV

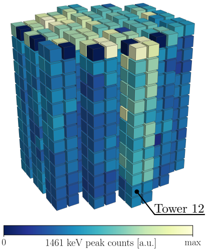

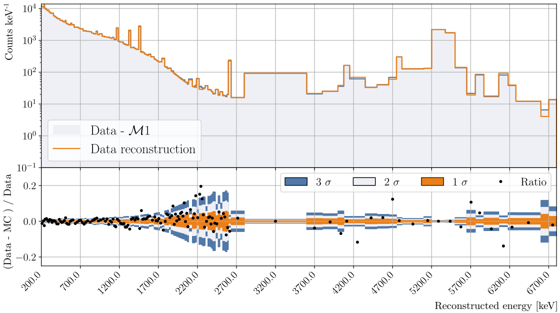

Exploit high granularity of CUORE to study space (and time) dependence of backgrounds

Phys. Rev. D 110, 052003 (2024)

S. Ghisandi Ph. D. Thesis

Results from the background model

- full reconstruction of data + estimate of activities of all background sources
- sensitivity levels down to 10 nBq kg^{-1} and 0.1 nBq cm^{-2} for bulk and surface contamination

Phys. Rev. D 110, 052003 (2024)

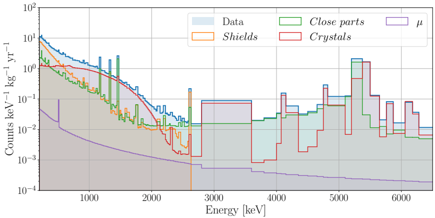

- measurement of 2νββ of ^{130}Te
  - dedicated analysis
  - component isolated from total spectrum

Source decomposition

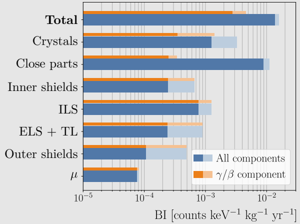

- reconstruction of BI
- benchmark for CUORE
- projections for CUPID
  - CUORE Upgrade with Particle IDentification
  - next-gen. 0νββ experiment

See talks by I. Nutini & P. Loaiza

Fit optimization for the 2νββ

- precise study of 2νββ spectral shape
  - privilege signal-to-background & goodness of fit
  - … over larger exposure
- ∼ 70% increase 2νββ events / background
- ×3 improvement of goodness of fit
  - subset of channels selected
    - innermost towers (7 out of 19)
    - detector self-shielding
  - optimized binning + energy range

Phys. Rev. Lett. 135, 082501 (2025)

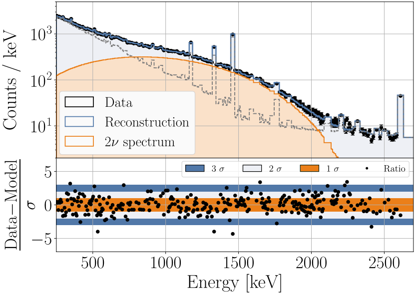

Choice of nuclear model

- select single-state dominance (SSD) as reference
  - leading contribution from 1^+ state of intermediate nucleus
- preferred to higher-state dominance (HSD) model
  - $\chi^2_{red} = 1.47$ vs. 1.51 (1339 d. o. f.)

2νββ half-life measurement

- $T^{2\nu}_{1/2} = \ln 2 \, \frac{N_A \;\; MT\,(\mathrm{TeO_2}) \;\; \mathrm{i.a.}\,(^{130}\mathrm{Te})}{M_{mol}\,(^{130}\mathrm{Te})} \, \frac{\epsilon}{N^{2\nu}_{obs}}$
- Bayesian fit to data
  - statistical uncertainty (68% CI around mode) is $O(0.5\%)$
  - contribution from various parameters is negligible $O(0.01\%)$
  - multiple sources of systematic uncertainties included ($< 1\%$)

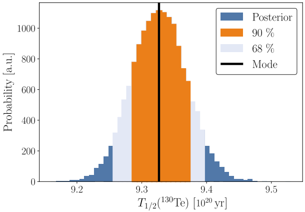

$$T^{2\nu}_{1/2} = 9.32 \; ^{+0.05}_{-0.04} \; (\mathrm{stat.}) \; ^{+0.07}_{-0.07} \; (\mathrm{syst.}) \; \times 10^{20} \; \mathrm{yr}$$

Twofold improvement on measurement precision

Phys. Rev. Lett. 135, 082501 (2025)

Systematic uncertainties

Class	Value (%)
Energy threshold	$^{+0.146}_{-0}$
Binning	$^{+0.160}_{-0.068}$
Dataset	$^{+0.594}_{-0.594}$
Geometry	$^{+0.350}_{-0.350}$
Bremsstrahlung	$^{+0.160}_{-0.162}$
Total	$^{+0.740}_{-0.711}$

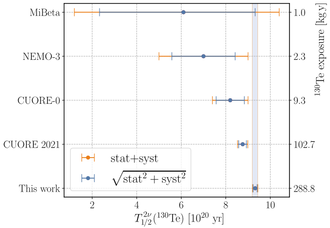

Improved formalism

CUORE

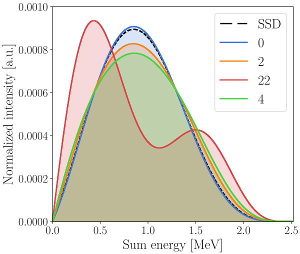

- SSD model provides excellent fit to experimental data
- **however** 2νββ shape is fixed *a priori*
  - fit does not support nuclear model refinement
- use of improved formalism
  - Taylor expansion over lepton energies
  - calculation of subleading nuclear matrix elements (NMEs)
  - spectral shapes + relative strengths can be extracted from fit
- constraints on intermediate states
- test effective value of axial coupling constant g_A^{eff} in nuclear medium

$$\left[T_{1/2}^{2\nu}\right]^{-1} = \left(g_A^{\text{eff}}\right)^4 \left|M_{GT}^{2\nu}\right|^2 G_{SSD}$$

$$\longrightarrow \quad \left[T_{1/2}^{2\nu}\right]^{-1} = \left(g_A^{\text{eff}}\right)^4 \left|M_{GT-1}^{2\nu}\right|^2 \left\{ G_0 + \xi_{31} G_2 + \frac{1}{3}\left(\xi_{31}\right)^2 G_{22} + \left[\frac{1}{3}\left(\xi_{31}\right)^2 + \xi_{51}\right] G_4 + \frac{1}{3}\xi_{31}\xi_{51} G_{42} + \frac{2}{3}\xi_{31}\xi_{51} G_6 \right\}$$

Expanded decomposition

$$\left[T^{2\nu}_{1/2}\right]^{-1} = \left(g_A^{\text{eff}}\right)^4 \left|M^{2\nu}_{GT-1}\right|^2 \left\{ G_0 + \xi_{31} G_2 + \frac{1}{3}\left(\xi_{31}\right)^2 G_{22} + \left[\frac{1}{3}\left(\xi_{31}\right)^2 + \xi_{51}\right] G_4 + \frac{1}{3}\xi_{31}\xi_{51} G_{42} + \frac{2}{3}\xi_{31}\xi_{51} G_6 \right\}$$

- G_0, G_2, G_{22}, G_4, G_{42} and G_6 are phase space factors (PSFs)
- $M^{2\nu}_{GT-1}$, $M^{2\nu}_{GT-3}$, and $M^{2\nu}_{GT-5}$ are NME expansion terms
  - GT stands for Gamow-Teller transition
- define ratios $\xi_{31} \equiv M^{2\nu}_{GT-3}/M^{2\nu}_{GT-1}$ and $\xi_{51} \equiv M^{2\nu}_{GT-5}/M^{2\nu}_{GT-1}$
  - ξ_{31} and ξ_{51} provide complementary insights into decay process
  - $M^{2\nu}_{GT-1}$ sensitive to contributions from high-lying states in intermediate odd-odd nucleus
  - $M^{2\nu}_{GT-3}$ and $M^{2\nu}_{GT-5}$ primarily determined by lowest-energy states
- study of ξ_{31} and ξ_{51} also probes HSD model $\rightarrow$ requires $\xi_{31} = \xi_{51} = 0$

- data reconstruction with multiple shape components for 2νββ
  - spectrum templates weighted for PSFs (fixed) + normalization factors (flat priors)
  - $\mathcal{L}(MC \mid \text{data}) = \prod_k \prod_i \mathcal{P}(\nu_{k,i} \mid n_{k,i})$ where $\nu_i = \sum_j f^j \, s^j_{MC,i}$ (f = norm, s_{MC} = counts)
  - improved formalism: $f^{2\nu} \, s^{2\nu}_{MC} \rightarrow \sum_t G_t \, f^{2\nu}_t \cdot s^{2\nu}_{MC,t}$
- theoretical computation for PSFs and NMEs
  - PSFs: screened exact finite-size Coulomb wave functions
  - NME templates: proton-neutron quasi-particle random-phase approximation
  - include radiative and atomic exchange corrections for emitted electrons
    - affect both the PSFs and the spectral shape
    - largest impact below the fit threshold
    - measurable shift for maximum of spectrum

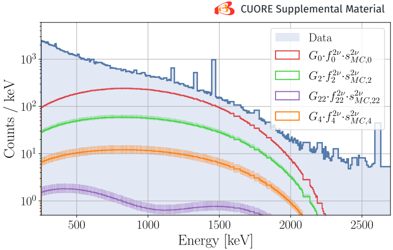

Results from the fit

- good fit to CUORE data
  - reduced chi-square $\chi^2_{\text{red}} = 1.48$ (1337 d.o.f.)
  - compatibility with SSD $< 1\sigma$ across entire energy range
  - SSD model slightly favored
    - lower number of parameters + weaker correlations
  - extracted half-life consistent $< 1\sigma$
    - if systematic on model: contribution of -0.53%
- considerations on nuclear models
  - ξ_{31} consistent with 0 ($\xi_{31} < 0.5$ @90% $C.I.$)
  - non-zero ξ_{51} $\Rightarrow$ 4 th-order NME > over 2 nd-order NME
    - HSD ruled out at $> 5\sigma$
    - extremely high anti-correlation ($\rho = -0.78$)
  - discrepancy from theoretical predictions
    - incomplete description of decay (neglected minor effects)
    - potential BSM physics

Need further theoretical studies & more precise experimental determination of spectral shape

Posterior distributions

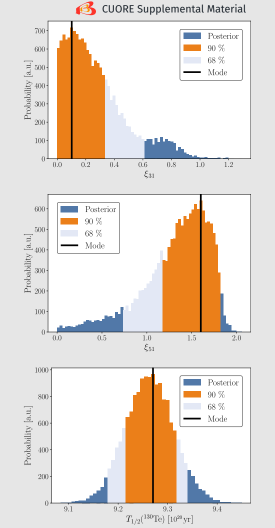

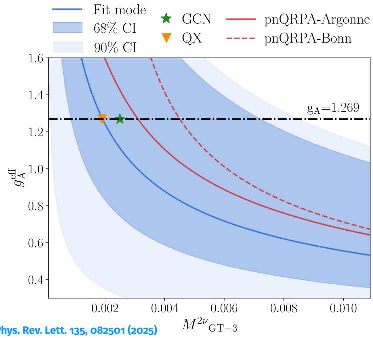

Phys. Rev. Lett. 135, 082501 (2025)

$$g_A^{eff} = \left[\frac{\left[T_{1/2}^{2\nu\beta\beta}\right]^{-1} \cdot \xi_{31}^2}{M_{GT-3}^2 \cdot G} \right]^{1/4}$$

$$G = G_0 + \xi_{31} G_2 + \frac{1}{3}\xi_{31}^2 G_{22} + \left(\frac{1}{3}\xi_{31}^2 + \xi_{51}\right) G_4$$

PRL 131, 162501 (2023)

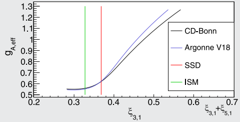

PRL 122, 192501 (2019)

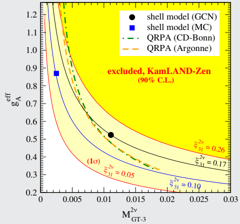

First-ever information from ^{130}Te on g_A and NMEs

- relatively high uncertainty
  - smaller S/N wrt to similar studies on ^{100}Mo and ^{136}Xe
  - advanced background model + high collected statistics
- mode confirming quenching of g_A
- good match with theoretical models

Summary

- most precise measurement of ^{130}Te 2νββ half-life obtained by CUORE
  - twofold improvement from complete background model + optimization of data selection
  - $t^{2\nu}_{1/2} = 9.32\ ^{+0.05}_{-0.04}\ \text{(stat.)}\ ^{+0.07}_{-0.07}\ \text{(syst.)}\ \times 10^{20}$ yr
- first study of 2νββ shape for ^{130}Te within improved formalism
  - constraints on effective value of g_A thanks to higher signal-to-background + background model
  - preference for SSD over HSD model (excluded at $> 5\sigma$)
- nuclear matrix element ξ_{31} meets theoretical predictions / ξ_{51} is far away
  - discrepancy maybe from incomplete description of the decay or potential BSM physics
  - … motivates further theoretical studies + even more precise measurement

Thank you!

CUORE Collaboration – LNGS (Italy), May 2024

The CUORE Collaboration thanks the directors and staff of the Laboratori Nazionali del Gran Sasso and the technical staff of our laboratories. This work was supported by the Istituto Nazionale di Fisica Nucleare (INFN); the National Science Foundation under Grants No. NSF-PHY-0605119, No. NSF-PHY-0500337, No. NSF-PHY-0855314, No. NSF-PHY-0902171, No. NSF-PHY-0969852, No. NSF-PHY-1307204, No. NSF-PHY-1314881, No. NSF-PHY-1401832, and No. NSF-PHY-1913374; Yale University; Johns Hopkins University; and University of Pittsburgh. This material is also based upon work supported by the U.S. Department of Energy (DOE) Office of Science under Contracts No. DE-AC02-05CH11231 and No. DE-AC52-07NA27344; by the DOE Office of Science, Office of Nuclear Physics under Contracts No. DE-FG02-08ER41551, No. DE-FG03-00ER41138, No. DE-SC0012654, No. DE-SC0020423, and No. DE-SC0019316. This research used resources of the National Energy Research Scientific Computing Center (NERSC). This work makes use of both the DIANA data analysis and APOLLO data acquisition software packages, which were developed by the CUORICINO, CUORE, LUCIFER, and CUPID-0 Collaborations. The authors acknowledge Advanced Research Computing at Virginia Tech for providing computational resources and technical support that have contributed to the results reported within this paper.

Systematic uncertainties

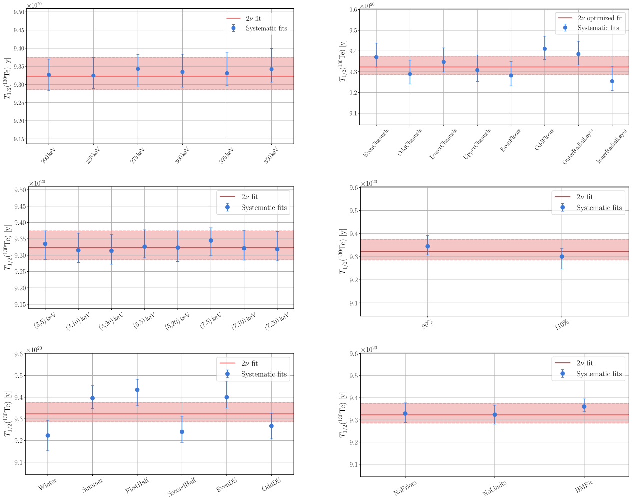

Class	Value (%)
Energy threshold	$^{+0.146}_{-0}$
Binning	$^{+0.160}_{-0.068}$
Dataset	$^{+0.594}_{-0.594}$
Geometry	$^{+0.350}_{-0.350}$
Bremsstrahlung	$^{+0.160}_{-0.162}$
Total	$^{+0.740}_{-0.711}$

CUORE Supplemental Material

$$T^{2\nu}_{1/2} = 9.32\ ^{+0.05}_{-0.04}\ (\text{stat.})\ ^{+0.07}_{-0.07}\ (\text{syst.})\ \times 10^{20}\ \text{yr}$$

CUORE bulk contamination

Contaminant	Prior [Bq kg^{-1}]		Mode/Limit [Bq kg^{-1}]	Systematic
Crystals				
^{130}Te $2\nu\beta\beta$			$(3.03 \pm 0.01) \times 10^{-5}$	$^{+0.11}_{-0.17}$
^{232}Th	$< 1.2 \times 10^{-7}$	CUORE-0	$(2.75 \pm 0.05) \times 10^{-7}$	$^{+0.85}_{-1.47}$
^{228}Ra $\to$ ^{208}Pb	$< 7.5 \times 10^{-8}$	CUORE-0	$(1.19 \pm 0.04) \times 10^{-7}$	$^{+0.2}_{-1.16}$
^{238}U $\to$ ^{230}Th	$< 3.6 \times 10^{-8}$	CUORE-0	$< 6.36 \times 10^{-10}$	
^{230}Th	$(2.8 \pm 0.3) \times 10^{-7}$	CUORE-0	$(3.85 \pm 0.06) \times 10^{-7}$	$^{+0.26}_{-1.3}$
^{226}Ra $\to$ ^{210}Pb	$< 2.2 \times 10^{-8}$	CUORE-0	$< 4.63 \times 10^{-10}$	
^{210}Pb	$(1.37 \pm 0.83) \times 10^{-6}$	CUORE-0	$(1.55 \pm 0.02) \times 10^{-6}$	$^{+0.44}_{-1.48}$
^{235}U $\to$ ^{231}Pa			$< 2.92 \times 10^{-11}$	
^{231}Pa $\to$ ^{207}Pb			$< 9.06 \times 10^{-10}$	
^{190}Pt	$(1.95 \pm 0.05) \times 10^{-6}$	CUORE-0	$(1.93 \pm 0.01) \times 10^{-6}$	$^{+0.29}_{-0.3}$
^{147}Sm			$(1.09 \pm 0.12) \times 10^{-8}$	$^{+0.67}_{-0.58}$
^{125}Sb			$(2.93 \pm 0.11) \times 10^{-6}$	$^{+2.42}_{-1.44}$
^{110m}Ag			$(9.06 \pm 2.44) \times 10^{-8}$	$^{+62.58}_{-2.45}$
^{108m}Ag			$(6.02 \pm 1.08) \times 10^{-8}$	$^{+2.61}_{-2.66}$
^{60}Co	$(3.0 \pm 1.4) \times 10^{-7}$	CUORE-0	$(1.86 \pm 1.22) \times 10^{-8}$	$^{+4.21}$
^{40}K (no T12)	$< 8.2 \times 10^{-6}$	CUORE-0	$(4.30 \pm 0.12) \times 10^{-6}$	$^{+2.62}_{-1.11}$
^{40}K (T12)			$(2.45 \pm 0.68) \times 10^{-5}$	$^{+1.49}_{-0.63}$
Close parts				
^{232}Th	$< 2.1 \times 10^{-6}$	CUORE-0	$< 3.88 \times 10^{-7}$	
^{238}U	$< 2.2 \times 10^{-5}$	CUORE-0	$< 4.73 \times 10^{-7}$	
^{235}U			$< 2.17 \times 10^{-8}$	
^{137}Cs	$< 2.2 \times 10^{-5}$	HPGe	$(1.25 \pm 0.24) \times 10^{-6}$	$_{-0.71}$
^{60}Co	$< 2.5 \times 10^{-5}$	HPGe	$(2.04 \pm 0.03) \times 10^{-5}$	$^{+0.32}_{-0.39}$
^{54}Mn	$< 3.1 \times 10^{-5}$	HPGe	$(2.29 \pm 0.33) \times 10^{-6}$	$^{+2.63}_{-1.93}$
^{40}K			$(4.42 \pm 0.06) \times 10^{-4}$	$_{-1.06}$
Inner shields				
^{232}Th	$< 6.4 \times 10^{-5}$	HPGe	$(4.10 \pm 0.39) \times 10^{-5}$	$^{+1.92}_{-2.54}$
^{238}U	$< 5.4 \times 10^{-5}$	HPGe	$(7.71 \pm 5.03) \times 10^{-6}$	$^{+16.51}$
^{137}Cs			$< 1.92 \times 10^{-6}$	
^{60}Co	$< 2.4 \times 10^{-5}$	HPGe	$(1.46 \pm 0.19) \times 10^{-5}$	$^{+4.89}_{-1.44}$
^{54}Mn			$< 3.71 \times 10^{-6}$	
^{40}K	$< 6.7 \times 10^{-4}$	HPGe	$< 3.48 \times 10^{-5}$	

Contaminant	Prior [Bq kg^{-1}]		Mode/Limit [Bq kg^{-1}]	Systematic
Outer shields				
^{232}Th			$< 2.45 \times 10^{-5}$	
^{238}U			$< 4.02 \times 10^{-5}$	
^{137}Cs			$< 7.33 \times 10^{-4}$	
^{60}Co			$(1.45 \pm 0.04) \times 10^{-3}$	$^{+0.29}_{-0.87}$
^{54}Mn			$< 2.14 \times 10^{-4}$	
^{40}K			$< 8.61 \times 10^{-4}$	
ILS				
^{232}Th	$(3.9 \pm 2.2) \times 10^{-5}$	CUORE-0	$(1.70 \pm 0.22) \times 10^{-5}$	$^{+0.62}_{-0.8}$
^{238}U	$(2.7 \pm 1.0) \times 10^{-5}$	CUORE-0	$< 1.61 \times 10^{-6}$	< 11.44
^{108m}Ag			$(7.99 \pm 0.78) \times 10^{-6}$	$^{+2.62}_{-3.72}$
^{40}K			$< 3.87 \times 10^{-5}$	< 18.58
TL				
^{232}Th			$(3.06 \pm 1.47) \times 10^{-4}$	$^{+22.95}_{-2.74}$
^{238}U	$< 1.1 \times 10^{-3}$	HPGe	$(3.45 \pm 0.36) \times 10^{-3}$	$_{-3.44}$
^{210}Bi $\to$ ^{206}Pb			$(1.61 \pm 0.02) \times 10^{+2}$	$^{+0.51}_{-0.41}$
^{40}K	$< 7.6 \times 10^{-3}$	HPGe	$(3.74 \pm 2.64) \times 10^{-3}$	$^{+7.49}_{-3.01}$
ELS				
^{210}Bi			$(3.31 \pm 0.14) \times 10^{+2}$	$^{+1.35}_{-1.86}$
^{207}Bi			$(2.29 \pm 0.20) \times 10^{-3}$	$^{+1.21}_{-1.47}$

Phys. Rev. D 110, 052003 (2024)

Contaminant	Depth [μm]	Mode/Limit [Bq cm^{-2}]	Systematic
Crystals			
^{210}Pb	0.001	$(7.32 \pm 0.02) \times 10^{-8}$	$^{+4.98}_{-3.23}$
^{232}Th	0.01	$(3.10 \pm 0.14) \times 10^{-10}$	$^{+0.2}_{-2.98}$
^{228}Ra $\rightarrow$ ^{208}Pb	0.01	$(1.10 \pm 0.03) \times 10^{-9}$	$^{+0.69}_{-0.19}$
^{238}U $\rightarrow$ ^{230}Th	0.01	$(1.90 \pm 0.03) \times 10^{-9}$	$_{-1.08}$
^{230}Th	0.01	$(8.22 \pm 0.32) \times 10^{-10}$	$^{+13.51}_{-0.4}$
^{226}Ra $\rightarrow$ ^{210}Pb	0.01	$(2.56 \pm 0.04) \times 10^{-9}$	$^{+1.52}_{-1.12}$
^{235}U $\rightarrow$ ^{231}Pa	0.01	$(8.74 \pm 0.01) \times 10^{-10}$	$_{-0.50}$
^{231}Pa $\rightarrow$ ^{207}Pb	0.01	$(1.05 \pm 0.34) \times 10^{-10}$	$^{+1.07}_{-0.66}$
^{232}Th	0.1	$(3.21 \pm 1.52) \times 10^{-11}$	$^{+3.21}$
^{228}Ra $\rightarrow$ ^{208}Pb	0.1	$(5.34 \pm 0.34) \times 10^{-10}$	$_{-5.27}$
^{238}U $\rightarrow$ ^{230}Th	0.1	$(9.15 \pm 2.65) \times 10^{-11}$	$^{+36.50}_{-8.35}$
^{230}Th	0.1	$(8.64 \pm 2.56) \times 10^{-11}$	$^{+7.75}_{-3.98}$
^{226}Ra $\rightarrow$ ^{210}Pb	0.1	$(9.10 \pm 0.40) \times 10^{-10}$	$^{+1.31}_{-8.71}$
^{210}Pb	0.1	$(1.31 \pm 0.01) \times 10^{-8}$	$^{+0.29}_{-0.17}$
^{235}U $\rightarrow$ ^{231}Pa	0.1	$(4.21 \pm 1.22) \times 10^{-12}$	$^{+16.78}_{-3.84}$
^{231}Pa $\rightarrow$ ^{207}Pb	0.1	$< 6.06 \times 10^{-11}$	
^{232}Th	1	$(7.77 \pm 1.74) \times 10^{-11}$	$_{-3.81}$
^{228}Ra $\rightarrow$ ^{208}Pb	1	$(1.86 \pm 0.19) \times 10^{-10}$	$^{+10.17}_{-1.06}$
^{238}U $\rightarrow$ ^{230}Th	1	$(2.84 \pm 0.14) \times 10^{-10}$	$^{+0.51}_{-1.11}$
^{230}Th	1	$(9.32 \pm 1.84) \times 10^{-11}$	$^{+18.73}_{-5.25}$
^{226}Ra $\rightarrow$ ^{210}Pb	1	$(3.08 \pm 0.15) \times 10^{-10}$	$^{+1.41}_{-2.58}$
^{210}Pb	1	$(5.15 \pm 0.10) \times 10^{-9}$	$^{+0.7}_{-0.94}$
^{235}U $\rightarrow$ ^{231}Pa	1	$(1.31 \pm 0.06) \times 10^{-11}$	$^{+0.23}_{-0.51}$
^{231}Pa $\rightarrow$ ^{207}Pb	1	$< 2.23 \times 10^{-11}$	
^{232}Th	10	$(1.18 \pm 0.28) \times 10^{-10}$	$^{+7.12}$
^{228}Ra $\rightarrow$ ^{208}Pb	10	$(3.29 \pm 1.27) \times 10^{-11}$	$^{+61.54}$
^{238}U $\rightarrow$ ^{230}Th	10	$< 1.99 \times 10^{-11}$	
^{230}Th	10	$(2.17 \pm 0.25) \times 10^{-10}$	$^{+5.95}_{-0.78}$
^{226}Ra $\rightarrow$ ^{210}Pb	10	$(1.82 \pm 0.86) \times 10^{-11}$	$^{+10.24}_{-1.46}$
^{210}Pb	10	$(2.23 \pm 0.09) \times 10^{-9}$	$^{+2.48}_{-2.18}$
^{235}U $\rightarrow$ ^{231}Pa	10	$< 9.15 \times 10^{-12}$	
^{231}Pa $\rightarrow$ ^{207}Pb	10	$< 1.37 \times 10^{-11}$	

Contaminant	Depth [μm]	Mode/Limit [Bq cm^{-2}]	Systematic
Close parts			
^{232}Th	0.01	$(1.35 \pm 0.06) \times 10^{-9}$	$^{+0.51}_{-0.51}$
^{238}U	0.01	$(1.24 \pm 0.07) \times 10^{-9}$	$^{+0.44}_{-0.68}$
^{210}Pb	0.01	$(3.40 \pm 0.02) \times 10^{-7}$	$^{+1.22}_{-0.96}$
^{210}Pb	0.1	$(6.48 \pm 0.25) \times 10^{-8}$	$_{-3.55}$
^{235}U	0.01	$(5.71 \pm 0.03) \times 10^{-10}$	$^{+0.20}_{-0.31}$
^{210}Pb	1	$(5.23 \pm 0.19) \times 10^{-8}$	$^{+3.15}_{-0.69}$
^{232}Th	10	$(1.15 \pm 0.05) \times 10^{-8}$	$^{+0.34}_{-0.64}$
^{238}U	10	$(8.35 \pm 0.68) \times 10^{-9}$	$_{-3.96}$
^{210}Pb	10	$(6.85 \pm 0.69) \times 10^{-8}$	$^{+4.88}_{-4.23}$
^{235}U	10	$(3.84 \pm 0.31) \times 10^{-10}$	$_{-1.82}$
MC			
^{232}Th	0.01	$< 4.36 \times 10^{-9}$	
^{238}U	0.01	$(6.79 \pm 1.32) \times 10^{-8}$	$_{-6.42}$
^{210}Pb	0.01	$< 2.05 \times 10^{-5}$	< 17.11
^{235}U	0.01	$(3.12 \pm 0.61) \times 10^{-9}$	$_{-2.95}$
HEX			
^{210}Pb		$(8.23 \pm 0.20) \times 10^{-4}$	$^{+6.43}_{-6.43}$

Phys. Rev. D 110, 052003 (2024)